

Performance Analysis of AFDM with Multiple Antennas in Doubly Selective Channels

Haoran Yin, Jiaojiao Xiong, Yanqun Tang*

School of Electronics and Communication Engineering, Sun Yat-sen University, China

email: {yinh6@mail2, xiongjj7@mail2, tangyq8@mail}.sysu.edu.cn

Abstract—On the heels of orthogonal time frequency space (OTFS) modulation, the recently discovered affine frequency division multiplexing (AFDM) is a promising waveform for the sixth-generation wireless network. With the superiorities of high multiplexing and diversity gain of multiple-input multiple-output (MIMO), we formulate the vectorized input-output relationship of MIMO-AFDM system. Correspondingly, we derive the diversity order of MIMO-AFDM system in doubly dispersive channels. Furthermore, we propose an efficient single pilot aided with reduced guard (SPA-RG) symbols scheme to perform channel estimation in the discrete affine Fourier transform (DAFT) domain. It is worth emphasizing that MIMO-AFDM can achieve full diversity in doubly selective channels. Simulation results show that it has the bit error ratio (BER) performance similar to MIMO-OTFS in large frame size. Additionally, compared to ideal channel state information, our proposed SPA-RG scheme is verified to induce only marginal BER performance loss with the least overhead.

Index Terms—MIMO-AFDM, DAFT domain, doubly selective channels, channel estimation, message passing detection.

I. INTRODUCTION

The sixth-generation wireless network is envisioned to provide ultra-reliable, high data rate and low latency communications in high mobility scenarios, including vehicle-to-vehicle (V2V), unmanned aerial vehicles (UAV) and high-speed trains, etc.. These dynamic channels therein are characterized by heavy delay-Doppler spreads, which cast a huge challenge to the current widely adopted waveforms, such as orthogonal frequency division multiplexing (OFDM). The non-negligible Doppler shift devastates greatly the orthogonality between the subcarriers in OFDM, which is a serious problem especially in the case of higher frequency bands used in the future communication systems.

Many efforts have been made to design a new modulation waveform to accommodate time- and frequency-selective channels. An alternative two-dimensional modulation waveform named orthogonal time frequency space (OTFS) outperforms OFDM significantly [1], [2]. However, OTFS suffers from heavy guard overhead when conducting the pilot aided channel estimation [3]. Affine frequency division multiplexing (AFDM), a newly discovered waveform, always attains full diversity in doubly selective channels. Its strong paths separability guarantees a thorough delay-Doppler channel representation [4], [5]. Information symbols in AFDM are

multiplexed on a set of orthogonal chirps via inverse *discrete affine Fourier transform* (DAFT) [6], [7]. Numerical results in [4], [5] show that AFDM has the identical remarkable bit error ratio (BER) performance in doubly selective channels just as OTFS while possessing the advantage on fewer channel estimation overhead.

Multiple-input multiple-output (MIMO) techniques have been exploited to enhance the spectral and energy efficiency compared to single-input single-output (SISO) system. MIMO-OFDM has come to great success in the past and present wireless networks. Several works on MIMO-OTFS, including channel estimation and signal detection, have been well investigated [8], [9]. A single pilot aided scheme is introduced for the channel estimation of MIMO-AFDM system and AFDM based multiuser system in [10] from the perspectives of feasibility and simplicity. However, to the best of our knowledge, a comprehensive introduction to MIMO-AFDM system has not been established in the literature.

Our contributions can be summarized as follows. We first formulate the vectorized input-output relationship of MIMO-AFDM system. Based on that, we derive the diversity order of MIMO-AFDM system in doubly selective channels. Moreover, a novel channel estimation scheme, named single pilot aided with reduced guard (SPA-RG), is proposed to reduce the estimation overhead to the greatest extent. We compare the BER performance of MIMO-OFDM, MIMO-OTFS and MIMO-AFDM systems in practical frame size with message passing (MP) detector. Numerical results validate that MIMO-AFDM inherits the full diversity characteristic from SISO-AFDM in doubly selective channels. Furthermore, MIMO-AFDM is found to outperform MIMO-OFDM significantly and show great BER performance similarity compared to MIMO-OTFS.

The rest of this paper is organized as follows. Section II reviews the basic concepts of AFDM and introduces MIMO-AFDM system, which lays the foundations for its diversity order analysis in Section III and the development of channel estimation scheme in Section IV. Simulation results are presented in Section V, followed by the conclusions in Section VI.

II. AFDM SYSTEM

In this section, the basic concepts of AFDM from [4], [5] are reviewed. Based on that, we derive the vectorized input-output relationship of MIMO-AFDM system.

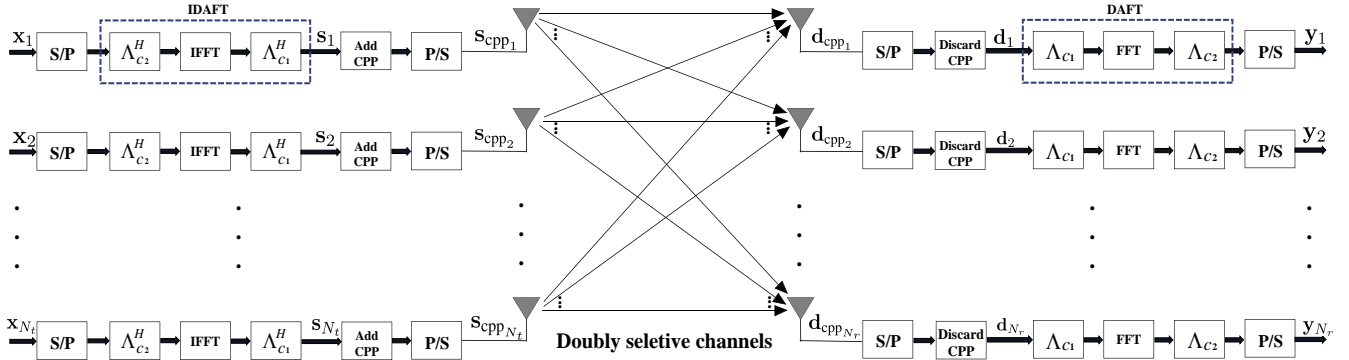


Fig. 1. $N_t \times N_r$ MIMO-AFDM modulation/demodulation block diagrams

A. SISO-AFDM system

1) AFDM Modulation: Let $\mathbf{x} \in \mathbb{A}^{N \times 1}$ denotes a vector of N quadrature amplitude modulation (QAM) symbols that reside on the DAFT domain, \mathbb{A} represents the modulation alphabet. After the serial to parallel operation, N points inverse DAFT (IDAF) is performed to convert \mathbf{x} to the time domain as

$$s[n] = \frac{1}{\sqrt{N}} \sum_{m=0}^{N-1} x[m] e^{j2\pi(c_2 m^2 + \frac{1}{N} mn + c_1 n^2)} \quad (1)$$

with $n = 0, \dots, N-1$ denoting the index of subcarriers, c_1 and c_2 being the AFDM parameters which will be illustrated later. The equation (1) can be rewritten in matrix form as

$$\mathbf{s} = \mathbf{\Lambda}_{c_1}^H \mathbf{F}^H \mathbf{\Lambda}_{c_2}^H \mathbf{x} = \mathbf{A}^H \mathbf{x} \quad (2)$$

where $\mathbf{A} = \mathbf{\Lambda}_{c_2} \mathbf{F} \mathbf{\Lambda}_{c_1}$ represents the DAFT matrix, $\mathbf{\Lambda}_c = \text{diag}(e^{-j2\pi c n^2}, n = 0, 1, \dots, N-1)$, \mathbf{F} is the DFT matrix with entries $e^{-j2\pi mn/N} / \sqrt{N}$. Before transmitting \mathbf{s} into the channel, a chirp-periodic prefix (CPP) should be added with a length greater than or equal to the maximum delay spread of the wireless channel. Assume the doubly selective channel has the following impulse response at time n and delay l

$$g_n(l) = \sum_{i=1}^P h_i e^{-j2\pi \frac{\alpha_i}{N} n} \delta(l - l_i) \quad (3)$$

where P is the number of paths, h_i is the channel gain, $l_i \in [0, l_{max}]$ and $\alpha_i \in [-\alpha_{max}, \alpha_{max}]$ are the delay and Doppler normalized with sample period and subcarrier spacing respectively. While in this paper, we consider $l_i \in \mathbb{Z}^+$ and $\alpha_i \in \mathbb{Z}^1$.

2) AFDM Demodulation: The received time domain symbols \mathbf{d}_{cpp} can be expressed as

$$d_{cpp}[n] = \sum_{l=0}^{\infty} s_{cpp}[n-l] g_n(l) + v[n] \quad (4)$$

where $v \sim \mathcal{CN}(0, N_0)$ represents the noise in time domain. After serial to parallel operation and discarding CPP, the

relationship between the CPP-free time domain symbols at the transmitter and receiver can be vectorized as

$$\mathbf{d} = \sum_{i=1}^P h_i \tilde{\mathbf{H}}_i \mathbf{s} + \mathbf{v} = \tilde{\mathbf{H}} \mathbf{s} + \mathbf{v} \quad (5)$$

with time domain subchannel matrix $\tilde{\mathbf{H}}_i = \mathbf{\Gamma}_{\text{CPP}_i} \mathbf{\Delta}_{\frac{\alpha_i}{N}} \mathbf{\Pi}^{l_i}$, $\mathbf{\Pi}$ denoting the forward cyclic-shift matrix, digital frequency shift matrix $\mathbf{\Delta}_{\frac{\alpha_i}{N}} \triangleq \text{diag}(e^{-j2\pi \frac{\alpha_i}{N} n}, n = 0, 1, \dots, N-1)$, and CPP matrix $\mathbf{\Gamma}_{\text{CPP}_i}$ being a $N \times N$ diagonal matrix

$$\mathbf{\Gamma}_{\text{CPP}_i} = \text{diag} \left(\begin{cases} e^{-j2\pi c_1 (N^2 - 2N(l_i - n))} & n < l_i \\ 1 & n \geq l_i \end{cases} \right) \quad (6)$$

$n = 0, \dots, N-1$. Finally, N points DAFT are implemented and the received time domain symbols \mathbf{d} is transformed to DAFT domain symbols \mathbf{y} with

$$y[m] = \frac{1}{\sqrt{N}} \sum_{n=0}^{N-1} d[n] e^{-j2\pi(c_2 m^2 + \frac{1}{N} mn + c_1 n^2)} + w[m] \quad (7)$$

where w represents the noise in DAFT domain and the corresponding matrix representation is

$$\mathbf{y} = \mathbf{\Lambda}_{c_2} \mathbf{F} \mathbf{\Lambda}_{c_1} \mathbf{d} = \mathbf{A} \mathbf{d}. \quad (8)$$

3) Input-Output Relationship: Substituting (1) (3) (4) into (7), we have the input-output relationship in DAFT domain as

$$y[p] = \sum_{i=1}^P h_i e^{j\frac{2\pi}{N} (N c_1 l_i^2 - q l_i + N c_2 (q^2 - p^2))} x[q] + w[p] \quad (9)$$

where $0 \leq p \leq N-1$, $q = (p + \text{loc}_i)_N$, $\text{loc}_i \triangleq \alpha_i + 2N c_1 l_i$. Similarly, the matrix form of (9) can be obtained by substituting (2) (5) into (8)

$$\mathbf{y} = \sum_{i=1}^P h_i \mathbf{H}_i \mathbf{x} + \mathbf{w} = \mathbf{H}_{\text{eff}} \mathbf{x} + \mathbf{w} \quad (10)$$

with DAFT domain subchannel matrix $\mathbf{H}_i = \mathbf{A} \tilde{\mathbf{H}}_i \mathbf{A}^H$, $\mathbf{H}_{\text{eff}} = \mathbf{A} \tilde{\mathbf{H}} \mathbf{A}^H$ being the effective channel matrix which possesses a sparse structure. As proven in [5] (Theorem 1), when c_1 is set to $\frac{2\alpha_{max}+1}{2N}$ and c_2 is either an arbitrary irrational number or a rational number sufficiently smaller than $\frac{1}{2N}$, AFDM can achieve full diversity in doubly selective channels.

¹The extension to the fractional delay and Doppler will be considered in our future work.

B. MIMO-AFDM system

We next introduce MIMO-AFDM system with its modulation/demodulation block diagrams provided in Figure.1. Let N_t and N_r denote the number of transmit antennas (TA) and receive antennas (RA) respectively. Then the linear model based input-output relationship between the r -th RA and N_t TAs in a $N_t \times N_r$ MIMO-AFDM system can be derived from (9) as

$$y_{r,p} = \sum_{t=1}^{N_t} \sum_{i=1}^{P_{r,t}} h_i^{r,t} e^{j \frac{2\pi}{N} (N \tilde{c}_1 (l_i^{r,t})^2 - q l_i^{r,t} + N c_2 (q^2 - p^2))} x_{t,q} + w_{r,p} \quad (11)$$

where $0 \leq p \leq N-1$, integers $r \in [1, N_r]$ and $t \in [1, N_t]$ denote the index of the RAs and TAs respectively, $q = (p + \text{loc}_i^{r,t})_N$ and $\text{loc}_i^{r,t} \triangleq \alpha_i^{r,t} + 2N \tilde{c}_1 l_i^{r,t}$, $P_{r,t} \geq 1$ is the number of paths between the r -th RA and the t -th TA, $h_i^{r,t}$ is the channel gain of the i -th path, $l_i^{r,t} \in [0, l_{max}^{r,t}]$ and $\alpha_i^{r,t} \in [-\tilde{\alpha}_{max}, \tilde{\alpha}_{max}]$ are the corresponding delay and Doppler shift respectively, $\tilde{\alpha}_{max}$ is the maximum Doppler among all pairs of RA and TA, and $\tilde{c}_1 = \frac{2\tilde{\alpha}_{max}+1}{2N}$. Then the matrix form of the input-output relationships between all pairs of RA and TA can be denoted as

$$\begin{aligned} \mathbf{y}_1 &= \mathbf{H}_{1,1} \mathbf{x}_1 + \mathbf{H}_{1,2} \mathbf{x}_2 + \cdots + \mathbf{H}_{1,N_t} \mathbf{x}_{N_t} + \mathbf{w}_1 \\ \mathbf{y}_2 &= \mathbf{H}_{2,1} \mathbf{x}_1 + \mathbf{H}_{2,2} \mathbf{x}_2 + \cdots + \mathbf{H}_{2,N_t} \mathbf{x}_{N_t} + \mathbf{w}_2 \\ &\vdots \\ \mathbf{y}_{N_r} &= \mathbf{H}_{N_r,1} \mathbf{x}_1 + \mathbf{H}_{N_r,2} \mathbf{x}_2 + \cdots + \mathbf{H}_{N_r,N_t} \mathbf{x}_{N_t} + \mathbf{w}_{N_r} \end{aligned} \quad (12)$$

with $\mathbf{H}_{r,t} = \mathbf{A} \tilde{\mathbf{H}}_{r,t} \mathbf{A}^H$ representing the effective channel matrix between the r -th RA and the t -th TA, $\tilde{\mathbf{H}}_{r,t}$ being the associated time domain channel matrix, noise vector $\mathbf{w} \sim \mathcal{CN}(\mathbf{0}, N_0 \mathbf{I})$. For the sake of compactedness, we define the effective MIMO channel matrix for the above MIMO-AFDM system as

$$\mathbf{H}_{\text{MIMO}} = \begin{bmatrix} \mathbf{H}_{1,1} & \mathbf{H}_{1,2} & \cdots & \mathbf{H}_{1,N_t} \\ \mathbf{H}_{2,1} & \mathbf{H}_{2,2} & \cdots & \mathbf{H}_{2,N_t} \\ \vdots & \vdots & \ddots & \vdots \\ \mathbf{H}_{N_r,1} & \mathbf{H}_{N_r,2} & \cdots & \mathbf{H}_{N_r,N_t} \end{bmatrix}_{N N_r \times N N_t} \quad (13)$$

where $\mathbf{H}_{\text{MIMO}} \in \mathbb{C}^{N N_r \times N N_t}$, the transmitted vector $\mathbf{x}_{\text{MIMO}} = [\mathbf{x}_1^T, \mathbf{x}_2^T, \dots, \mathbf{x}_{N_t}^T]^T \in \mathbb{C}^{N N_t \times 1}$, received vector $\mathbf{y}_{\text{MIMO}} = [\mathbf{y}_1^T, \mathbf{y}_2^T, \dots, \mathbf{y}_{N_r}^T]^T \in \mathbb{C}^{N N_r \times 1}$, and noise vector $\mathbf{w}_{\text{MIMO}} = [\mathbf{w}_1^T, \mathbf{w}_2^T, \dots, \mathbf{w}_{N_r}^T]^T \in \mathbb{C}^{N N_r \times 1}$. Then (12) can be rewritten as

$$\mathbf{y}_{\text{MIMO}} = \mathbf{H}_{\text{MIMO}} \mathbf{x}_{\text{MIMO}} + \mathbf{w}_{\text{MIMO}}. \quad (14)$$

III. DIVERSITY ANALYSIS OF MIMO-AFDM

In this section, we derive the diversity order of point-to-point MIMO-AFDM system in doubly selective channels. The channels between all pairs of RA and TA have the same delay-Doppler profile. According to (9), there are P non-zero elements in each row and column of $\mathbf{H}_{r,t}$ for $\forall r \in [1, N_r], t \in [1, N_t]$, each row of \mathbf{H}_{MIMO} has only $P N_t$ non-zero elements

and each column of \mathbf{H}_{MIMO} has only $P N_r$ non-zero elements. Therefore, (10) can be presented in an alternate way as [5]

$$\mathbf{y} = \sum_{i=1}^P h_i \mathbf{H}_i \mathbf{x} + \mathbf{w} = \tilde{\Phi}(\mathbf{x}) \tilde{\mathbf{h}} + \mathbf{w} \quad (15)$$

where $\tilde{\Phi}(\mathbf{x}) = [\mathbf{H}_1 \mathbf{x}, \mathbf{H}_2 \mathbf{x}, \dots, \mathbf{H}_P \mathbf{x}]_{N \times P}$, channel gain vector $\tilde{\mathbf{h}} = [h_1, h_2, \dots, h_P]^T \in \mathbb{C}^{P \times 1}$. Similarly, (14) can be rewritten as

$$\mathbf{Y} = \tilde{\Phi}(\mathbf{X}) \tilde{\mathbf{h}} + \mathbf{W} \quad (16)$$

where received symbol matrix $\mathbf{Y} = [\mathbf{y}_1, \mathbf{y}_2, \dots, \mathbf{y}_{N_r}]$ is an $N \times N_r$ matrix whose r -th column is the received symbol vector of the r -th RA, transmitted symbol matrix $\mathbf{X} = [\mathbf{x}_1, \mathbf{x}_2, \dots, \mathbf{x}_{N_t}]$ is an $N \times N_t$ matrix whose t -th column is the transmitted symbol vector of the t -th TA, $\tilde{\Phi}(\mathbf{X})$ is an $N \times P N_t$ concatenated matrix with definition of

$$\tilde{\Phi}(\mathbf{X}) = [\tilde{\Phi}(\mathbf{x}_1) \mid \tilde{\Phi}(\mathbf{x}_2) \mid \dots \mid \tilde{\Phi}(\mathbf{x}_{N_t})] \quad (17)$$

$\tilde{\mathbf{h}} \in \mathbb{C}^{P N_t \times N_r}$ is channel gain matrix with definition of

$$\tilde{\mathbf{h}} = \begin{bmatrix} \mathbf{h}_{1,1} & \mathbf{h}_{2,1} & \cdots & \mathbf{h}_{N_r,1} \\ \mathbf{h}_{1,2} & \mathbf{h}_{2,2} & \cdots & \mathbf{h}_{N_r,2} \\ \vdots & \vdots & \ddots & \vdots \\ \mathbf{h}_{1,N_t} & \mathbf{h}_{2,N_t} & \cdots & \mathbf{h}_{N_r,N_t} \end{bmatrix}_{P N_t \times N_r} \quad (18)$$

where $\mathbf{h}_{r,t} \in \mathbb{C}^{P \times 1}$ denotes the channel gain vector between the r -th RA and t -th TA, and its elements $h_i^{r,t}$ s are assumed to follow the distribution of $\mathcal{CN}(0, 1/P)$ (uniform scattering profile), $\mathbf{W} \in \mathbb{C}^{N \times N_r}$ is the noise matrix.

We normalize the transmitted symbol matrix \mathbf{X} so that the signal-to-noise ratio (SNR) per receive antenna is $\frac{1}{N_0}$. Let \mathbf{X}_i and \mathbf{X}_j be two transmitted symbol matrices. Assuming perfect channel state information and ML detection at the receiver, the probability of transmitting the symbol matrix \mathbf{X}_i and deciding in favor of \mathbf{X}_j at the receiver is the pairwise error probability (PEP) between \mathbf{X}_i and \mathbf{X}_j , which can be expressed as [11]

$$P(\mathbf{X}_i \rightarrow \mathbf{X}_j \mid \tilde{\mathbf{h}}, \mathbf{X}_i) = Q \left(\sqrt{\frac{\|(\tilde{\Phi}(\mathbf{X}_i) - \tilde{\Phi}(\mathbf{X}_j)) \tilde{\mathbf{h}}\|^2}{2N_0}} \right). \quad (19)$$

The PEP averaged over the channel statistics can be denoted as

$$P(\mathbf{X}_i \rightarrow \mathbf{X}_j) = \mathbb{E} \left[Q \left(\sqrt{\frac{\|(\tilde{\Phi}(\mathbf{X}_i) - \tilde{\Phi}(\mathbf{X}_j)) \tilde{\mathbf{h}}\|^2}{2N_0}} \right) \right]. \quad (20)$$

Let difference matrix $\delta^{(i,j)} \triangleq \mathbf{X}_i - \mathbf{X}_j$. The t -th column of $\delta^{(i,j)}$ is $\delta_t^{(i,j)} = \mathbf{x}_t^{(i)} - \mathbf{x}_t^{(j)}$, which denotes the difference of two transmitted symbols in the t -th TA. Since $\tilde{\Phi}$ is a linear operator, we have

$$P(\mathbf{X}_i \rightarrow \mathbf{X}_j) = \mathbb{E} \left[Q \left(\sqrt{\frac{\|\tilde{\Phi}(\delta^{(i,j)}) \tilde{\mathbf{h}}\|^2}{2N_0}} \right) \right]. \quad (21)$$

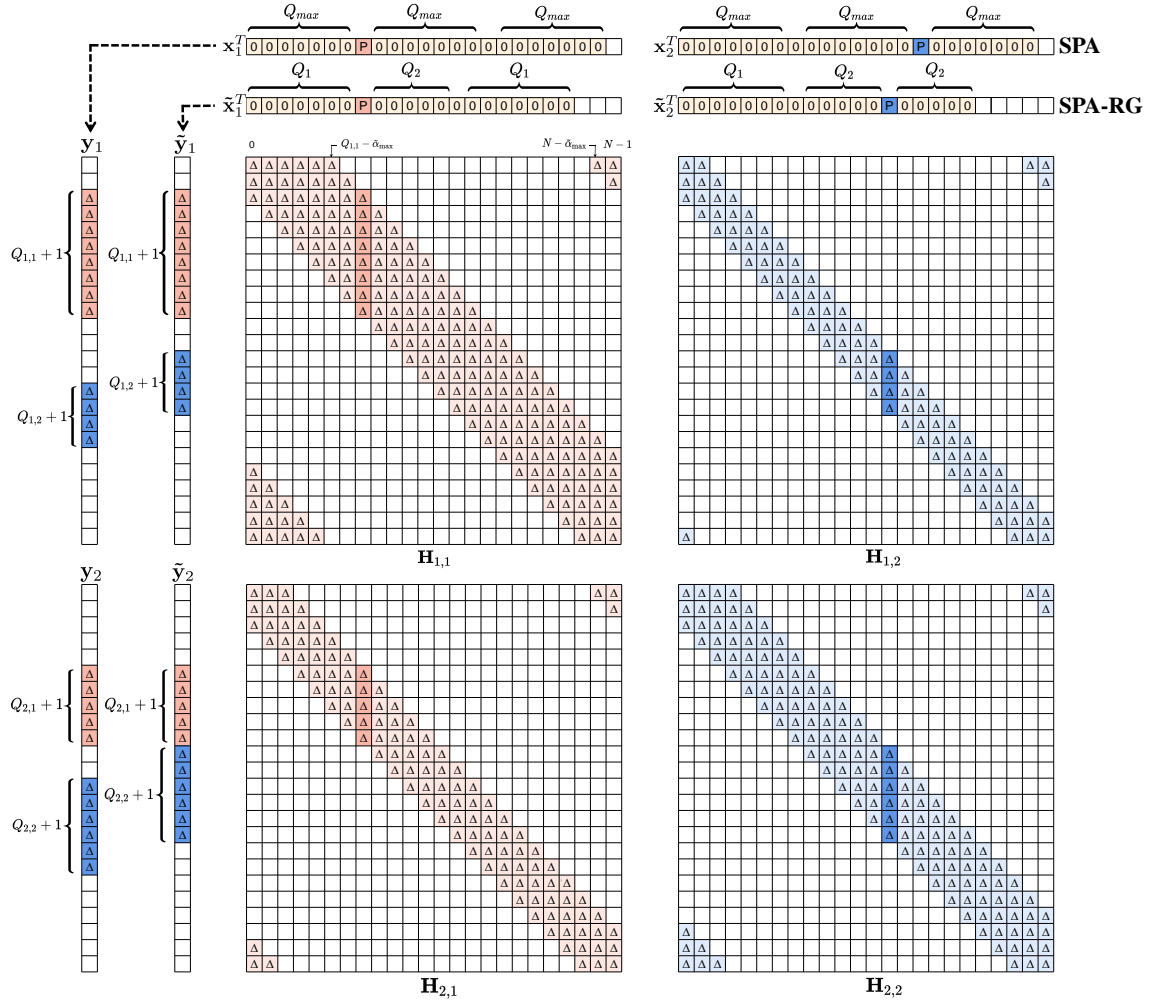


Fig. 2. SPA-RG and conventional SPA schemes for 2×2 MIMO-AFDM system. ('P':pilot, '0':guard, 'Δ': possible non-zero value)

Using Chernoff bound and the fact that each TA transmits independent AFDM symbols, an upper bound on the PEP in (21) can be obtained as [11]

$$P(\mathbf{X}_i \rightarrow \mathbf{X}_j) \leq \left(\prod_{l=1}^k \frac{1}{1 + \frac{\lambda_{t,l}^2}{4PN_0}} \right)^{N_r} \quad (22)$$

where $\lambda_{t,l}$ is the l -th singular value of the matrix $\Phi(\delta_t^{(i,j)})$ ($t \in 1, 2, \dots, N_t$) and k is the rank of $\Phi(\delta_t^{(i,j)})$. At high SNR value, (22) can be further simplified as

$$P(\mathbf{X}_i \rightarrow \mathbf{X}_j) \leq \frac{1}{N_o^{kN_r}} \left(\prod_{l=1}^k \frac{\lambda_{t,l}^2}{4P} \right)^{-N_r}. \quad (23)$$

We can observe from (23) that the exponent of the SNR term $\frac{1}{N_o}$ is kN_r , and the overall bit error ratio (BER) is dominated by the PEP with the minimum value of k , for all $i, j, i \neq j$. Therefore, the diversity order of MIMO-AFDM, denoted by ρ , is given by

$$\rho = N_r \cdot \min_{i,j,i \neq j} \text{rank}(\Phi(\delta_t^{(i,j)})). \quad (24)$$

In the APPENDIX A of [5], value $\min_{i,j,i \neq j} \text{rank}(\Phi(\delta_t^{(i,j)}))$ is proven to be P as long as the AFDM parameters c_1 and c_2 are tuned as we described in the end of Section II.A, and the number of subcarriers N satisfies

$$N \geq (l_{\max} + 1)(2\alpha_{\max} + 1). \quad (25)$$

Since $N \gg (l_{\max} + 1)(2\alpha_{\max} + 1)$ in practice, the diversity order of MIMO-AFDM is PN_r , which means MIMO-AFDM can achieve full diversity in doubly selective channels.

IV. CHANNEL ESTIMATION

In our prior work [10], we consider that the maximum delay $l_{\max}^{r,t}$ of the channels between all pairs of RA and TA are identical for simplicity, and a conventional single pilot aided (SPA) channel estimation scheme is proposed for point-to-point MIMO-AFDM system. However, this approximation results in spectral efficiency degradation in many scenarios, such as distributed MIMO and multiuser systems. Therefore, we relax that assumption in the following and propose a novel channel estimation scheme, named single pilot aided with reduced guard (SPA-RG). The SPA-RG scheme is performed in the

DAFT domain and consumes the minimum guard symbols (GS) among all the pilot based channel estimation schemes. A comparison between SPA-RG and SPA for a 2×2 MIMO-AFDM system is given in Figure.2.

Let's define $Q_{r,t} \triangleq (l_{\max}^{r,t} + 1)(2\tilde{\alpha}_{\max} + 1) - 1$, where $l_{\max}^{r,t}$ is the maximum delay between the r -th RA and the t -th TA, $Q_t = \max\{Q_{r,t} | r \in [1, N_r]\}$, $Q_{\max} = \max\{Q_t | t \in [1, N_t]\}$ and $S_t = \sum_{i=1}^t (1 + Q_i)$, $t \in [1, N_t]$. For each submatrix $\mathbf{H}_{r,t}$, as an example $\mathbf{H}_{1,1}$ shown in Figure.2, there are $Q_{r,t} + 1$ possible non-zero entries in all the columns corresponding to $Q_{r,t} + 1$ possible propagation paths [4], [10]. According to (11), the row and column coordinates of a non-zero entry in $\mathbf{H}_{r,t}$ are determined by the delay and Doppler of the associated path jointly, while the channel gain can be obtained from the value of the non-zero entry. Therefore, all the columns of $\mathbf{H}_{r,t}$ contain the same and intact CSI. Moreover, when N is sufficiently large, the CSIs between different RA and TA can be estimated at the same time by extracting the distinguish columns of the corresponding effective channel matrix with pilots and guard symbols.

To avoid interference between the received pilot symbols from different TAs at the receiver, the space between the pilots of $(t-1)$ -th TA and t -th TA should be larger than or equal to Q_t . Hence, we propose the following pilot and guard symbol arrangement for the t -th TA ($t = 1, \dots, N_t$)

$$x_t[m] = \begin{cases} \text{pilot} & m = S_t - 1 \\ \text{guard} & m \in [0, S_{N_t} + Q_t - 1]_N \\ & \text{and } m \neq S_t - 1 \\ \text{blank} & \text{otherwise} \end{cases} \quad (26)$$

where the overhead for channel estimation at the t -th TA is $O_t = S_{N_t} + Q_t$, and the total estimation overhead for an $N_t \times N_r$ MIMO-AFDM system applying the SPA-RG scheme can be expressed as

$$O_{\text{SPA-RG}} = \sum_{i=1}^{N_t} O_i = S_{N_t} N_t + \sum_{i=1}^{N_t} Q_i. \quad (27)$$

While the conventional SPA counterpart is $O_{\text{SPA}} = (Q_{\max} + 1)N_t^2 + Q_{\max}N_t$. By comparing the first and second parts of $O_{\text{SPA-RG}}$ and O_{SPA} respectively, we can conclude that without losing estimation accuracy, SPA-RG has the advantage on higher spectral efficiency over SPA. This improvement will be more prominent in ultra-high speed scenarios where the maximum Doppler $\tilde{\alpha}_{\max}$ is especially high, resulting in the difference enlargement between $O_{\text{SPA-RG}}$ and O_{SPA} . Based on the symbol arrangement in (26), N in SPA-RG should satisfy $S_{N_t} \leq N$. The left blank slots can be further explored to enhance the spectral efficiency by transmitting information symbols. In summary, by exploring the sparsity and circulation characteristics of each submatrix $\mathbf{H}_{r,t}$ flexibly, an efficient and simple channel estimation scheme for MIMO-AFDM system can be obtained.

V. SIMULATION RESULTS

In this section, we first present the BER performance of MIMO-AFDM with ML detection in small frame size and

TABLE I
SIMULATION PARAMETERS FOR AFDM

Parameter	Value
Carrier frequency f_c (GHz)	4
Number of subcarriers N_{AFDM} (frame size)	6, 1024
Subcarrier spacing Δf_{AFDM} (Hz)	1776, 444
Maximum UE speed (kmph)	480
Modulation scheme	BPSK
Detector	ML, MP

MP detection (proposed in [12]) in large frame size under the assumption of ideal CSI at the receiver. Then the performance of MIMO-AFDM with imperfect CSI is explored with the proposed SPA-RG channel estimation scheme. Each transmit antenna in MIMO configuration transmits independent information symbols. The channel gains of all the paths follow the distribution of $\mathcal{CN}(0, 1/P)$. The pilot signal for signal-to-noise ratio (SNR) is denoted as SNRp. Other parameters considered for the simulation are summarized in Table I.

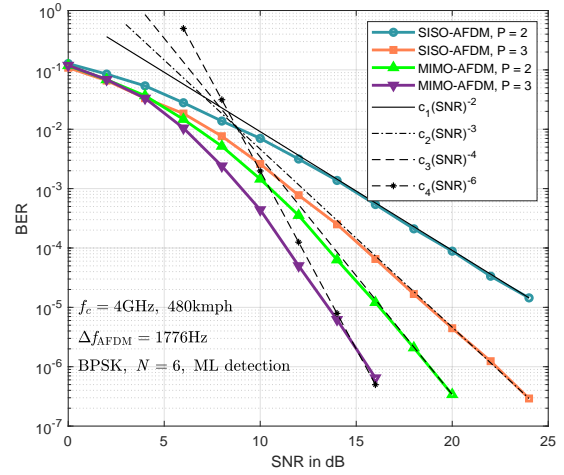


Fig. 3. BER performance of SISO-AFDM and 2×2 MIMO-AFDM systems with ideal CSI and ML detection.

Figure.3 shows the BER performance of SISO-AFDM and 2×2 MIMO-AFDM systems. $N_{\text{AFDM}} = 6$, $\Delta f_{\text{AFDM}} = 1776$ Hz and ML detection are used. The normalized delay-Doppler profile of channel with two paths is (0, 0) and (1, 1), while that corresponds to three paths is (0, 0), (0, 1) and (1, 1). Asymptotic lines with slopes of 2 ($c_1(\text{SNR})^{-2}$), 3 ($c_2(\text{SNR})^{-3}$), 4 ($c_3(\text{SNR})^{-4}$) and 6 ($c_4(\text{SNR})^{-6}$) are plotted. We can observe that the MIMO-AFDM system outperforms SISO-AFDM system thanks to the space diversity gain from multiple RAs. The multiple TAs of MIMO-AFDM bring in the advantages of linear increase in spectral efficiency with the number of TAs. Furthermore, the diversity orders achieved by SISO-AFDM in channels with two and three paths are 2 and 3 respectively, while the 2×2 MIMO-AFDM counterparts are 4 and 6 respectively, proving the validity of the diversity order derived in Section III.

Figure.4 shows the BER performance comparisons among SISO-AFDM, SISO-OTFS, MIMO-OFDM, MIMO-AFDM

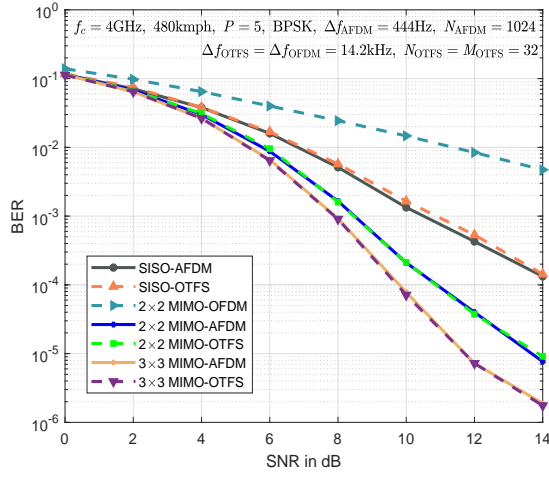


Fig. 4. BER comparisons among SISO-AFDM, SISO-OTFS, MIMO-OFDM, MIMO-AFDM and MIMO-OTFS systems with ideal CSI and MP detection.

and MIMO-OTFS systems with perfectly known CSI. $N_{\text{AFDM}} = 1024$, $\Delta f_{\text{AFDM}} = 444$ Hz and MP detection are used. OTFS subcarrier spacing $\Delta f_{\text{OTFS}} = \Delta f_{\text{OFDM}} = 14.2$ kHz and frame size $N_{\text{OTFS}} = M_{\text{OTFS}} = 32$ are adopted to ensure the same resources are occupied ($N_{\text{OTFS}} \times M_{\text{OTFS}} = N_{\text{AFDM}}$). $P = 5$ paths with normalized delay-Doppler profile of $(0, 0)$, $(1, 1)$, $(2, 2)$, $(3, 3)$, $(4, 4)$ are applied. We can observe that the 2×2 MIMO-AFDM system outperforms 2×2 MIMO-OFDM system significantly. This is because MIMO-OFDM suffers from severe inter-carrier interference caused by the heavy Doppler shifts. Moreover, owing to the equivalent delay-Doppler channel representation in DAFT domain, AFDM establishes nearly the same BER as OTFS in SISO and MIMO configurations with large frame size.

We next investigate the BER performance of 2×2 MIMO-AFDM system with estimated CSI. The SPA-RG scheme with different SNRp and MP detection are used. The same parameters as the last simulation are adopted. We can observe from Figure.5 that the BER performance enhances as SNRp increases since the larger energy of the pilots used, the more accurate CSI can be obtained. We can also notice that when SNRp reaches 30 dB, the BER of MIMO-AFDM system using the estimated CSI shows only marginal degradation compared to that with ideal CSI, which validates the effectiveness of the proposed SPA-RG scheme. Note that in practice, it is feasible to suppose a high SNRp value without violating the average transmit power constraint because the zeros guard symbols will balance the overall transmit energy.

VI. CONCLUSION

In this paper, a comprehensive introduction to the MIMO-AFDM system is presented. We derive the vectorized the input-output relationship and the diversity order of MIMO-AFDM in doubly selective channels. We also propose a novel and efficient channel estimation scheme in the DAFT domain to reduce the overhead to the greatest extent. Simulation results verify that MIMO-AFDM always achieve full diversity in dou-

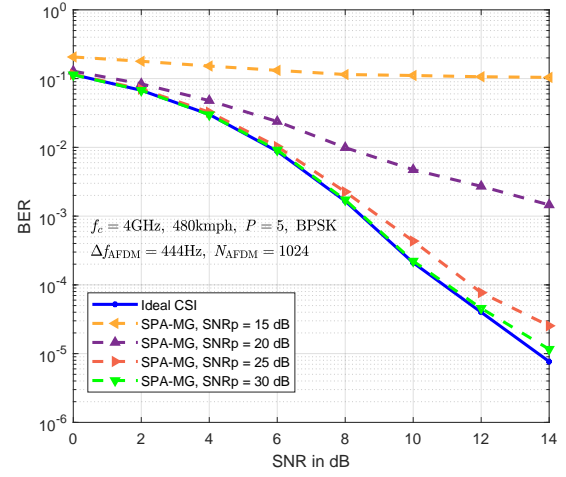


Fig. 5. BER versus SNR of 2×2 MIMO-AFDM system applying SPA-RG scheme with different SNRp and MP detection.

bly selective channels. Moreover, MIMO-AFDM outperforms MIMO-OFDM significantly while showing great performance similarity to MIMO-OTFS with MP detector. Finally, The proposed SPA-RG scheme can provide precise CSI for signal detection when the energy of pilot is large enough.

REFERENCES

- [1] R. Hadani, S. Rakib, M. Tsatsanis, A. Monk, A. J. Goldsmith, A. F. Molisch, and R. Calderbank, "Orthogonal time frequency space modulation," IEEE Wireless Communications and Networking Conference (WCNC), pp. 1-6, 2017.
- [2] G. D. Surabhi, R. M. Augustine, and A. Chockalingam, "On the diversity of uncoded OTFS modulation in doubly-dispersive channels," IEEE Transactions on Wireless Communications, vol. 18, no. 6, pp. 3049-3063, Jun. 2019.
- [3] P. Raviteja, K. T. Phan, and Y. Hong, "Embedded pilot-aided channel estimation for OTFS in delay-doppler channels," IEEE Transactions on Vehicular Technology, vol. 68, no. 5, pp. 4906-4917, 2019.
- [4] A. Bemani, N. Ksairi and M. Kountouris, "AFDM: a full diversity next generation waveform for high mobility communications," IEEE International Conference on Communications Workshops (ICC Workshops), pp. 1-6, 2021.
- [5] A. Bemani, N. Ksairi and M. Kountouris, "Affine frequency division multiplexing for next generation wireless communications," arXiv: 2204.12798, 2022.
- [6] S. Chang Pei and J. Jiu Ding, "Closed-form discrete fractional and affine Fourier transforms," IEEE Transactions on Signal Processing, vol. 48, no. 5, pp. 1338-1353, May 2000.
- [7] T. Erseghe, N. Laurenti, and V. Cellini, "A multicarrier architecture based upon the affine fourier transform," IEEE Transactions on Communications, vol. 53, no. 5, pp. 853-862, May 2005.
- [8] M. K. Ramachandran and A. Chockalingam, "MIMO-OTFS in high-doppler fading channels: signal detection and channel estimation," IEEE Global Communications Conference (GLOBECOM), pp. 206-212, 2018.
- [9] W. Shen, L. Dai, J. An, P. Fan and R. W. Heath, "Channel estimation for orthogonal time frequency space (OTFS) massive MIMO," IEEE Transactions on Signal Processing, vol. 67, no. 16, pp. 4204-4217, Aug. 2019.
- [10] H. Yin, Y. Tang, "Pilot aided channel estimation for AFDM in doubly dispersive channels," accepted by 2022 IEEE/CIC International Conference on Communications in China (ICCC 2022).
- [11] D. Tse and P. Viswanath, Fundamentals of Wireless Communication. Cambridge, U.K.: Cambridge University. Press, 2005.
- [12] P. Raviteja, K. T. Phan, Y. Hong, and E. Viterbo, "Interference cancellation and iterative detection for orthogonal time frequency space modulation," IEEE Transactions on Wireless Communications, vol. 17, no. 10, pp. 6501-6515, Oct. 2018.